EFFECT OF SOLIDIFICATION TIME ON THE MICROSTRUCTURE AND MECHANICAL PROPERTIES OF THE COMPACTED GRAPHITE IRON FOR HEAVY DUTY ENGINE BLOCKS

Evandro Hoepers
Tupy S.A. / Fundação Universidade do Estado de Santa Catarina

Carlos de Souza Cabezas
Tupy SA

Guilherme Ourique Verran
Fundação Universidade do Estado de Santa Catarina

ABSTRACT

The microstructure of compacted graphite iron, in addition to being influenced by factors such as chemical composition, liquid treatment and heat treatment, is strongly affected by the solidification time. That, during solidification, is mainly influenced by product section thickness, melting temperature and the ability of the mold material to absorb heat. However, the effect of that variable on the mechanical properties of different sections of the same part is rarely reported. In this study, the influence of the solidification time on the microstructure and mechanical properties of a compacted graphite iron class ISO16112/JV400 was evaluated from specimens extracted from specific regions of a heavy-duty engine block with section thicknesses varying from 6 to 50 mm. It was observed progressive increases of up to 100 MPa for the ultimate tensile strength and of up to 70 MPa for the yield strength with decreasing solidification time. With the set of results obtained, polynomial regression models were developed to predict the effect of solidification time on mechanical properties. In this way, subsidies are presented for designers to use more optimized mechanical properties data that will allow greater wall thickness reductions, resulting in better thermal exchanges and lighter components.

INTRODUCTION

Demands for increasingly compact engines that promote lower fuel consumption, reduced emissions and increased power and torque have guided the development of engine technology for many years. These performance improvements, in terms of efficiency and power density (kw/l or kw/kg), result in the need for components with greater thermal and mechanical resistance. [1] [2] [3].

To meet these needs, over the years, compact graphite iron (CGI) and aluminum compete to present continuous technological innovations that promote the most attractive conditions for their selection as a component material. While aluminum has lower density and higher thermal conductivity, CGI has greater fatigue resistance, stiffness and vibration dampening capacity, as well as stable mechanical resistance in higher operation temperatures. This makes possible, for example, to design engine blocks with smaller sizes in CGI and with lower final mass than those in aluminum. [1] [4]

However, the process to achieve thin-walled compacted graphite iron castings is complex, as the microstructure, in addition to being influenced by factors such as chemical composition, liquid treatment and heat treatment, is strongly affected by the cooling rate. [6] During solidification, the rate of cooling experienced by a given casting is primarily a function of the section size, melting temperature and the ability of the mold material to absorb heat. The increase in the cooling rate leads to smaller solidification times that have strong effect on the eutectic cell and graphite morphology, therefore, on the resulting mechanical properties. [5] [6]

For example, a decrease of the wall thickness from 25mm to 4mm can bring to an increase of nodularity from 4% to 20% and a decrease of the graphite size from 35µm to 15µm leading to an increase of the ultimate tensile strength and yield strength up to 70Mpa.[7] Nonetheless not often the thicker regions are the ones with bigger solidification times due the influence of product geometry and ingate system. [8] In this way the casting process simulation has proved in the last thirty years to be a reliable tool for solidification time definition. [9]

(Allowed reproduction with source mention: AEA – Simpósio Internacional de Engenharia Automotiva – SIMEA 2022 – São Paulo, Brasil)

Based on the downsizing approach and on CGI consolidated potential to be applied in engine blocks, this work presents the effect of solidification time, related to wall thickness and product geometry, on the microstructure and mechanical properties of a compacted graphite iron heavy duty engine block. The goal was to create a reliable data base for designers, allowing them to apply CGI in a more optimal way. The work presented here is part of the master thesis from one of the authors at UDESC.

EXPERIMENTAL PROCEDURES

The research of this work was carried out using the structure, resources, products, tools, and laboratories of the TUPY SA foundry, based in Joinville/SC.

The object of this study was a i6 300 kg engine block, cast in CGI class ISO16112/JV/400/U. It was select regions of this part with section thicknesses ranging from 6 mm to 50 mm, which guarantees different solidification times.

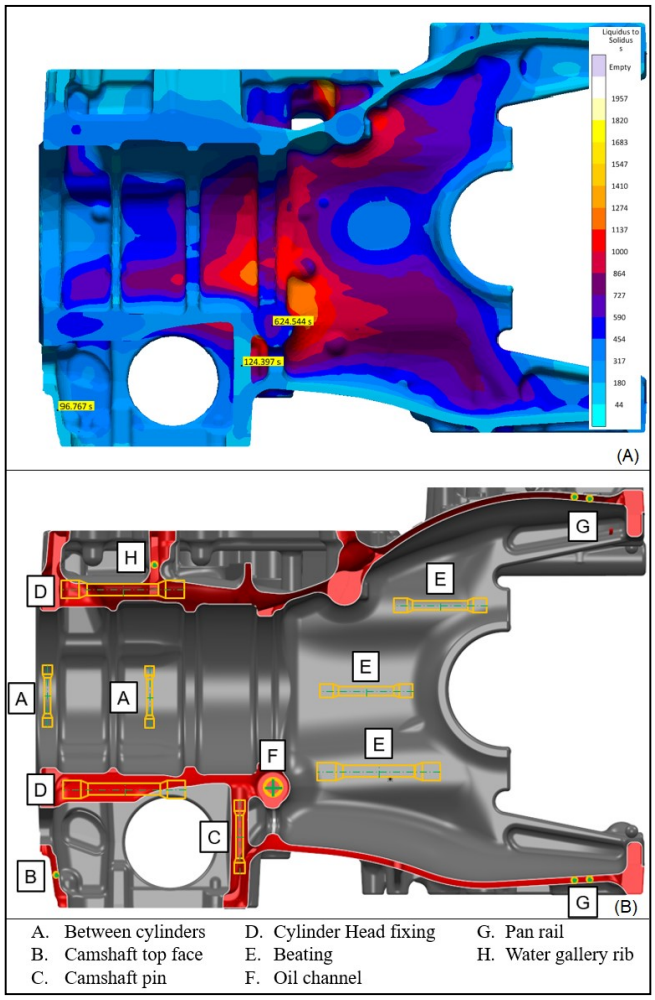

Figure 1. Engine block - Simulation and specimens.

The solidification process was simulated using Magmasoft® software, showed in Figure 1(A), which was used to capture the cooling curves. The Engine Block was sectioned to separate main bearing 2, 3 and 5, obtaining the cross-section showed in Figure 1 (B), indicating where the tensile specimens and solidification times were taken. The solidification times were defined trougth solidification curves from Magma simulation as ilustrated in Figure 2.

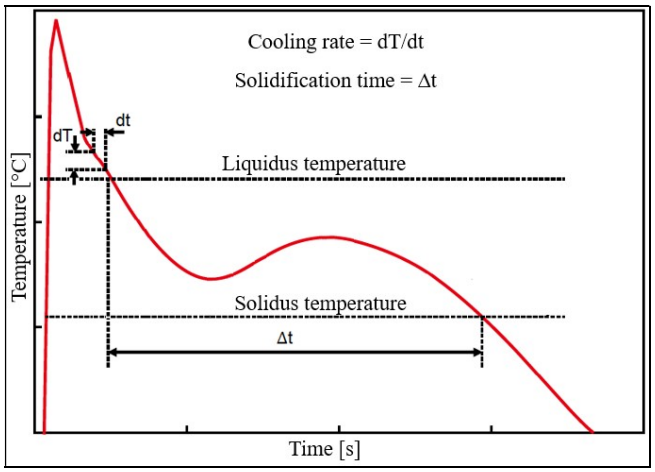

Figure 2. Solidification time definition.

It was selected two engine block from two diffeent cast batches. The first block was used to extract specimens for tensile test and microstructure analysis from all defined points, totaling 15 regions and 41 specimens and was used as a basis for analysis of the effect of solidification time on microstructure and mechanical properties of the component. The second engine block was used to validate the model. From this engine block it was taken specimens for tensile test and microstructure analysis from points with minimum and maximum solidification times, totaling 7 regions and 18 specimens.

The tensile test was carried in accordance with the standard DIN 50125:2009-07.

The chemical composition of this alloy is typical of CGI class ISO16112/JV/400/U, as shown in Table 2.

%C	%Si	%Sn	%Cu	%Mn
3,40	2,20	0,06	0,6	0,20
3,80	2,60	0,10	1,0	0,50

Table 1. Chemical Composition.

Microstructure characterization was performed analyzing the percentage of nodular graphite, percentage of ferrite in the matrix, pearlite microhardness and eutectic cell count.

The microstructure analysis was performed in the tensile specimens after mechanical tests according to the standards: ABNT NBR 13284:1995, ABNT NBR 6593:2015, EM16112:2017, ABNT NBR 8108:1983, ASTM A247-19 and EM6507-1:2018. For eutectic cell analysis, it was used Molz etching. [10]

RESULTS AND DISCUSSION

The results and discussions about the development of this work were divided as follows: Results of solidification simulation, Results of microstructure characterization, Results of mechanical tests, Comparative analysis between different cast batches and mechanical properties prediction through solidification time.

SOLIDIFICATION SIMULATION – As predicted in literature, higher cooling rates and shorter solidification times were observed in regions with thinner wall thickness. [6] Figure 3 shows the correlation between solidification time and wall thickness. It is important to notice that some regions with same wall thickness can present different solidification times. This is because of the effect of adjacent thicker regions that can impose a longer solidification time in nearby regions.

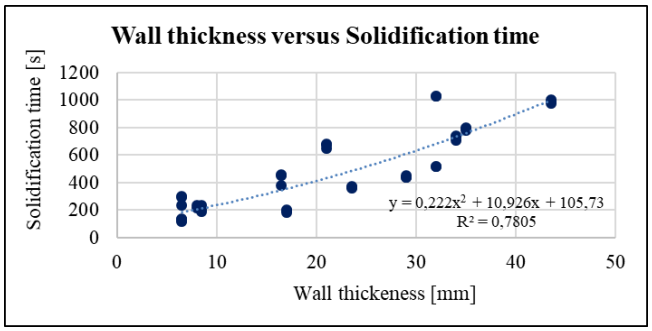

Figure 3. Wall thickness versus Solidification time.

MICROSTRUCTURE ANALYSIS - The nodularity range was between 7 to 20%. The correlation between solidification time and nodularity is shown in Figure 4. There was not a significant effect of solidification time on the percentage of nodular graphite.

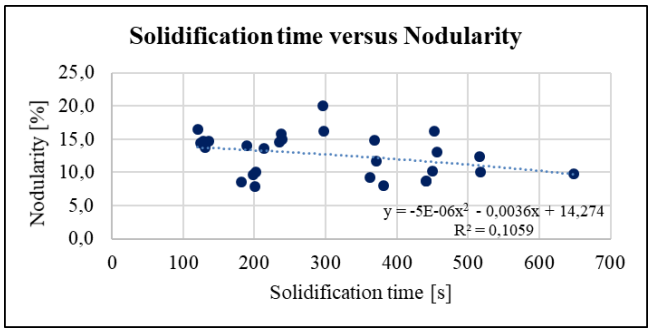

Figure 4. Solidification time versus Nodularity.

The ferrite content ranged from 2 to 4%. There was no significant effect of solidification time on the percentage of ferrite, probably to the tight range of nodularity achieved throughout the sections and the level of alloying elements used.

Microhardness changed subtly, from around 340 HV in shorter solidification time sections to around 315 HV in longer solidification time sections, as shown in Figure 5. This increase in average hardness can be explained by the refinement of pearlite for the shortest solidification time.

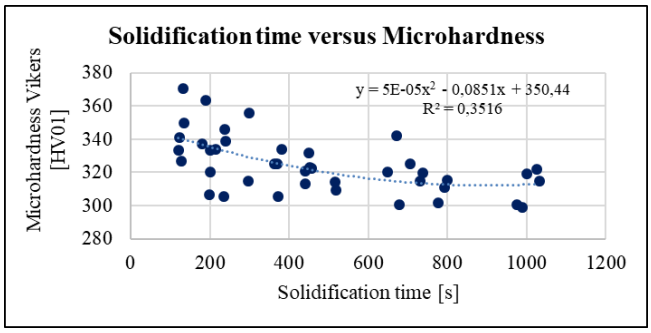

Figure 5. Solidification time versus Microhardness

The refinement of the microstructure was verified with the decrease of the solidification time observing an increase in the number of eutectic cells per unit of area for regions with shorter solidification times, when compared to regions with opposite conditions. Figure 6 shows the micrographs of the samples with different solidification times: blue regions represent a eutectic cell, whereas brownish areas are intercellular regions. There is a clear coarseness of the microstructure as the solidification time increases.

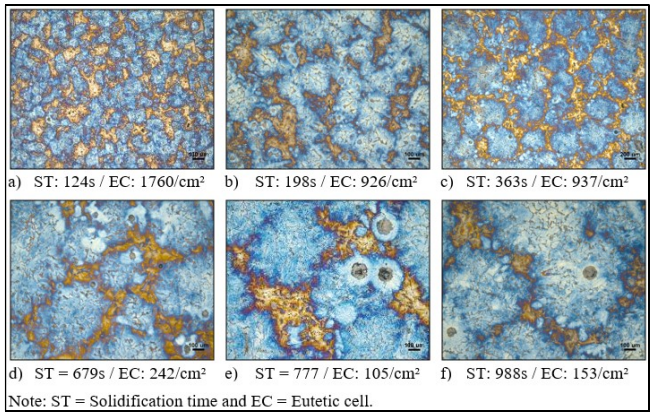

Figure 6. Micrographs with color etching (100x).

The effect of increasing solidification times on eutectic cell formation can also be seen on Figure 7. There was an increase of up to 10 times in the number of eutectic cells per square centimeter as the solidification time changes from 1000 to 180s. This is explained by the high number of active nuclei in fast solidification areas and segregation profile in longer solidification areas. [12] [13]

MECHANICAL PROPERTIES – A progressive increase in the Ultimate Tensile Strength (UTS) and in the Yield Strength (YS) was verified for thicknesses smaller than twenty millimeters as shown on Figure 8 and 9. However, there was a variation of up to 90 MPa in the UTS for equal thicknesses. This fact is explained by the product's thermal gradient, which increases the solidification time of thin regions close to large masses or even by a constant flow of hot metal caused by the feeding system. That is,

thin sections are not always a synonym for high solidification times. In this way, the correlation between wall thickness and mechanical properties is not as accurate as the correlation of mechanical properties and solidification time.

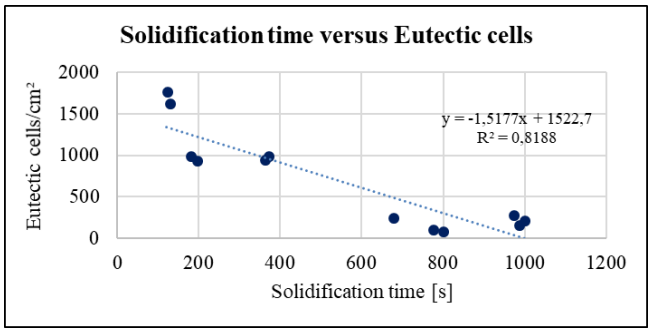

Figure 7. Solidification time versus Eutectic cells.

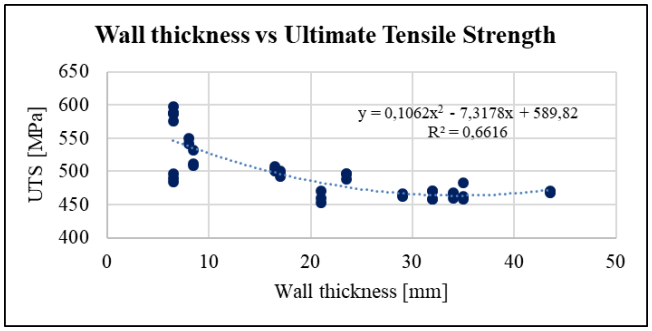

Figure 8: Wall thickness versus Ultimate tensile strength.

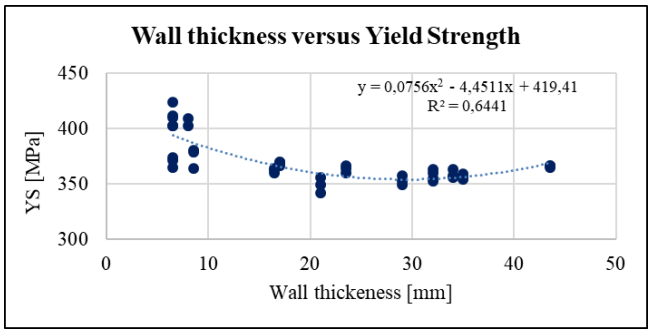

Figure 9: Wall thickness versus Yield Strength.

The better accuracy of the correlation of solidification time with Ultimate Tensile Strength is shown in Figure 10. A steep progressive increase in ultimate tensile strength was observed until 500s of solidification times. Above this limit the UTS reaches a plateau of around 450MPa. Comparing the longest solidification times to the shortest solidification times there is an increase of around 100MPa. That means that a standard CGI ISO16112/JV/400/U can reach almost 600 MPa in thinner sections with shorter solidification times.

The same tendency could be seen for the Yield Strength, as shown in Figure 11. A strong progressive increase in Yield Strength was observed until 500s of solidification time. Above this limit the YS reaches a plateau of around 350MPa. There is an increase of up to 70MPa for the shortest solidification times in relation to the longest solidification times.

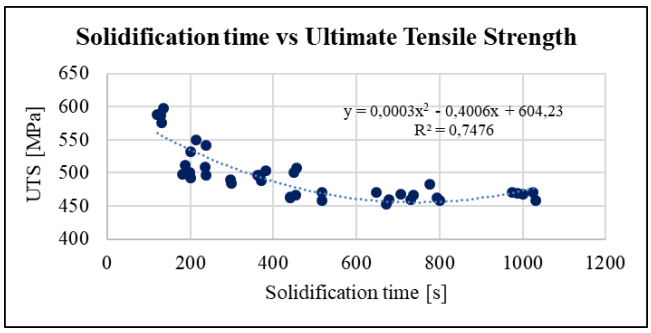

Figure 10: Solidification time versus UTS.

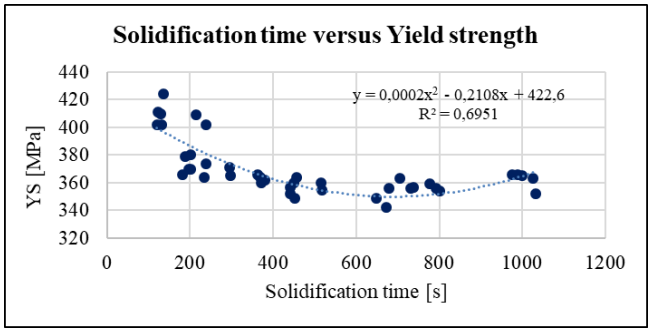

Figure 11: Solidification time versus YS.

To verify the effects of the microstructure on the mechanical properties, a multiple linear regression analysis was performed with all studied microstructure parameters. The variance analysis of the model indicated that only the eutectic cells/cm² had significant effect on the Ultimate Tensile Strength. Other parameters, such as nodularity, graphite particles/mm², %ferrite and microhardness did not have a significant effect, as they varied little for the different section thicknesses.

Figure 12 shows the positive effect of the increase in eutectic cells/cm² on the Ultimate Tensile Strength. This converges with the literature data, which shows that reducing the size of eutectic cells (or increasing the eutectic cell number), reduces the formation of fragile rupture planes, increasing the tensile strength. [14]

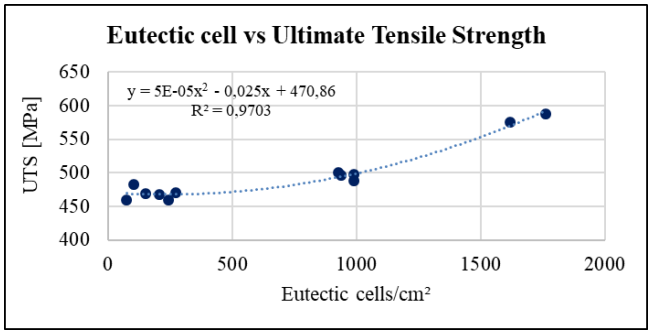

Figure 12. Eutectic cells versus UTS.

DIFFERENT CAST BATCHES - Figure 13 shows the correlation of solidification time with Ultimate Tensile Strength from the two engine blocks with different casting batches. It was verified a similar effect of the solidification time on the two engine bocks through the similarity of the angular coefficients of the tendency lines, -0.1028 for the first block and -0.0973 for the second block. The difference between the constants of the tendency line equations, which indicate a lower average strength resistance for the second block, is because the average percentage of nodularity of the second block (8.3% of nodularity) is lower than the first block (13.1% nodularity). The increase in nodularity has a strong effect on increasing the strength resistance of CGI. [7] The difference between the nodularities of the two blocks is due to normal variations in the nodularization treatment of the CGI casting process. [15]

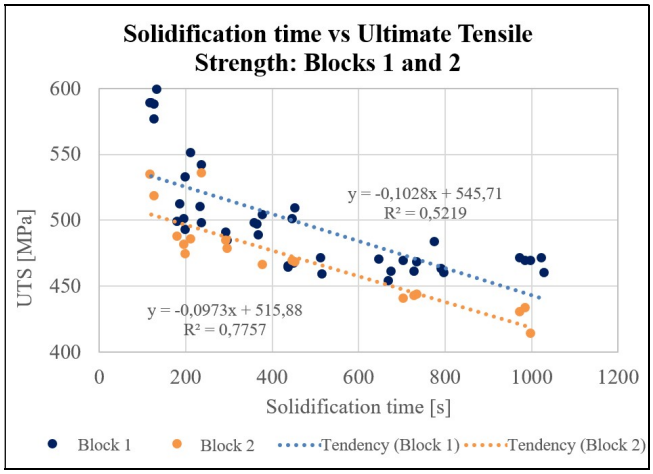

Figure 13. Different cast batches comparison.

MECHANICAL PROPERTIES PREDICTION THROUGH SOLIDIFICATION TIME – The models to predict the effect of solidification time on mechanical properties were developed using polynomial regression analyzes of Minitab® statistical software. For all models, the 95% confidence interval and the 95% prediction interval were calculated. The reciprocal data transformation (1/x) was adopted for the solidification time data to obtain the best fits of the models.

Figure 14 brings the polynomial regression model of the Ultimate Tensile Strength. Based on this model, it is possible to assume, with 95% confidence, that for solidification time equal to 125 seconds the Ultimate Tensile Strength will be within the range of 550MPa to 620MPa, while for solidification times equal to 1000 seconds the Ultimate Tensile Strength will be within the range of 430MPa to 500MPa.

Figure 15 shows the polynomial regression model for the Yield Strength. The model predicts that that for solidification time equal to 125 seconds the Yield Strength will be within the range of 390MPa to 435MPa, while for solidification times equal to 1000 seconds the Yield Strength will be within the range of 330MPa to 380MPa.

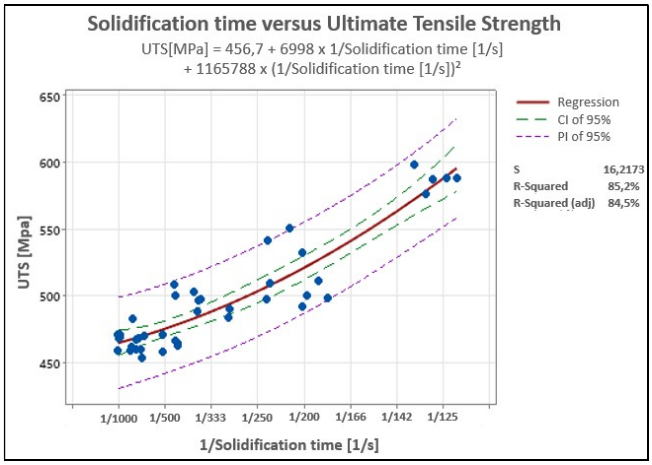

Figure 14. Prediction model for Ultimate Tensile Strength.

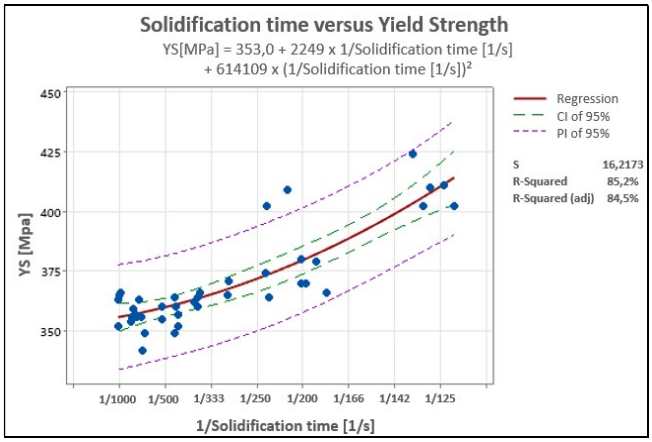

Figure 15. Prediction model for Yield Strength.

In order to verify the adherence of these models to different casting batches, the equations of the developed models were validated with the results of block number 2, after adjusting their constants due to differences in the average nodularity. Figures 16 and 17 show the good adherence to the models described.

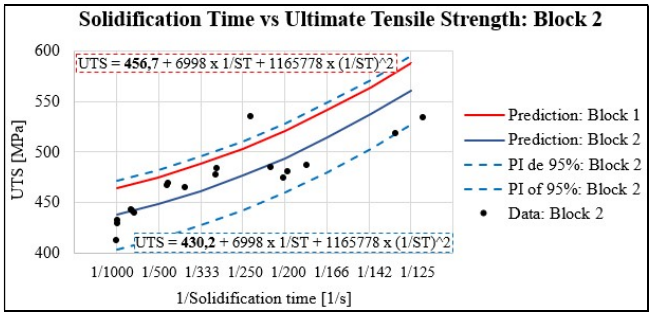

Figure 16. Prediction model of UTS applied to engine block 2.

In this way, the extension of the developed models for different cast batches, parts and classes of CGI is possible. Figure 18 summarizes the application of the developed models for different products or CGI classes using known

values of UTS, YS and Solidification time. The first step is to define the constants of the equations (β_0) by inserting in the constant equations ($\beta_{0(UTS^1,ST^1)}$ and $\beta_{0(YS^1,ST^1)}$) actual or desired values of UTS and YS from a section of the part with known solidification time. The second step is to plot the curves of the equations ($UTS_{(ST)}$ and $YS_{(ST)}$) with the defined constants. Thus, with a few tensile tests and a solidification simulation, it is possible to predict the Ultimate Tensile Strength and Yield Strength throughout the various sections of the part.

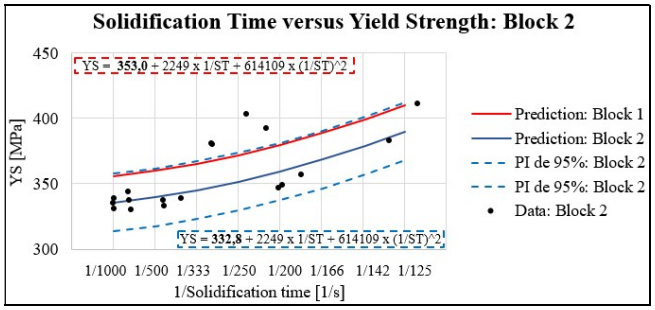

Figure 17. Prediction model of YS applied to engine block 2.

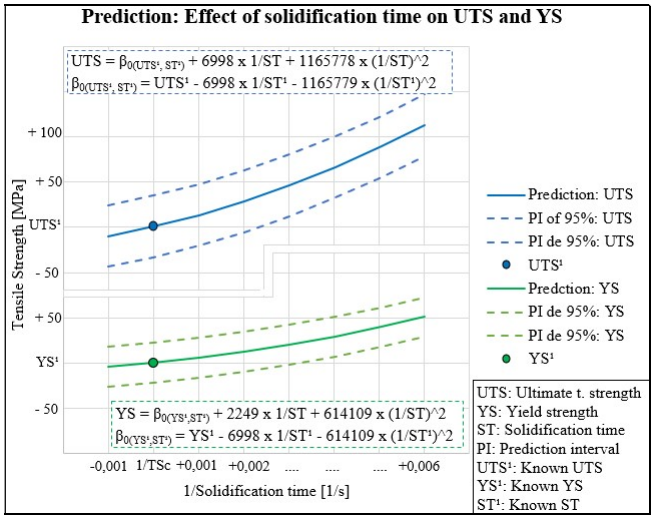

Figure 18. Prediction model for UTS and YS.

CONCLUSIONS

Based on the results achieved and discussions carried out in the development of this work, the conclusions were:

- No significant effect of solidification times on nodularity was observed.
- Refinement of perlite lamellae and a small increase in microhardness were observed for shorter solidification times.
- There was 10 times increase in the number of eutectic cells per square centimeter with a decrease in solidification time from 1000 seconds to 150 seconds.
- There was a progressive increase in the Ultimate Tensile Strength and Yield Strength from solidification times from 100 to 500 seconds. Above 500 seconds, the change in UTS and YS are much more subtle.
- The increase in UTS for the shortest solidification time (100s) in relation to the longest solidification times (above 500s) was up to 100 MPa
- The increase in YS for the shortest solidification time (100s) in relation to the longest solidification times (above 500s) was up to 70 MPa
- It was possible to predict the mechanical properties (U.T.S. and Y.S.) in different sections of the Engine Block, based on the solidification time through polynomial regression models with a confidence level of 95%.

BIBLIOGRAPHY

[1] GUESSER, W. L.; GUEDES, L.C. The new generation engines and the challenges for the foundry industry. XXIV Simpósio Internacional de Engenharia Automotiva, São Paulo, v. 3, n. 1., 2016.

[2] GUESSER, W.; SCHROEDER, T.; DAWSON, S. Production experience with compacted graphite iron automotive components. Journal: AFS Transactions, Illinois, v. 01-071, p. 1-11, 2011.

[3] DAWSON, S; INDRA, F. Compacted graphite iron: A new material for highly stressed cylinder blocks and cylinder heads. 28th International Vienna Motor Symposium, Germany, v. 2, p. 181-191, 2007.

[4] QIU, H.; CHEN, Z. The forty years of vermicular graphite cast iron development in China - (Part I). Journal: China foundry, China, v. 4, p. 91-98, 2007.

[5] GÓRNY, M. Cast iron: Compacted Graphite. In: TOTTEN, G. e COLÁS, R. Encyclopedia of iron, steel, and their alloys. 1. ed., Boca Raton: CRC Press, p. 718-735, 2016.

[6] GÓRNY, M.; KAWALEC, M.; SIKORA, G. Effect of cooling rate on microstructure of thin-walled vermicular graphite iron castings. Journal: Archives of Foundry Engineering, v. 14, n. 1/2014, p. 139-142, 2014.

[7] GUESSER, W. L. Propriedades Mecânicas dos Ferros Fundidos. São Paulo: Publisher: Edgard Blucher, 2009.

[8] GAMBA, Angelo Carlos. Influência das espessuras das seções nas microestruturas e nas propriedades mecânicas dos ferros fundidos vermiculares SiMo. Master teses – Universidade Estadual de Santa

Catarina. Programa de Pós-Graduação em Ciência e Engenharia de Materiais, Joinville, 2017.

[9] FLENDER, E.; STURM, J. Thirty years of casting process simulation. Journal: International Journal of Metalcasting, v. 4, n. 7-23, 2010.

[10] MOTZ, J. M.; Microsegregation: an easily unnoticed influencing variable in the structural description of cast materials. Journal: Praktische Metallographie, v. 25, n. 6, p. 285-293, 1988.

[11] CHAROENVILAISIRI, S.; STEFANESCU, M. D. Thin Wall Compacted Graphite Iron Castings. Journal: AFS Trasactions, v. 02-176, 2002.

[12] ELLIOTT, R. Cast iron technology. 1. ed., Manchester, England: Butterworth & Co., 1988

[13] KURZ M.; FISHER, D.J. Fundamentals of Solidification, 3. ed., Uetikon-Zuerich, Switzerland: Trans Tech Publications Ltd, 1992.

[14] GÓRNY, M. General characteristic of the ductile and compacted graphite cast iron. In: Microstructure and Properties of Ductile Iron and Compacted Graphite Iron Castings. SpringerBriefs in Materials. Switzerland: Publisher Springer, 2015.

[15] DAWSON, S. Process control for the production of compacted graphite iron. In: AFS Casting Congress, 2002, Kansas City. Available in: https://foundrygate.com/upload/artigos/